

Reappraisal of the asymptotic state of a zero pressure gradient turbulent boundary layer

Lyazid Djenidi

School of Engineering,
The University of Newcastle,
Newcastle, 2308 NSW Australia
lyazid.djenidi@newcastle.edu.au

Krishna M. Talluru

School of Civil Engineering,
The University of Sydney,
Sydney, NSW 2006, Australia
murali.talluru@Sydney.edu.au

Robert A. Antonia

School of Engineering,
The University of Newcastle,
Newcastle, 2308 NSW Australia
robert.antonio@newcastle.edu.au

ABSTRACT

In this paper we study a zero pressure gradient turbulent boundary layer developing over a two-dimensional rough wall that consists of a periodic arrangement of cylindrical rods with a spacing (p) of eight times the rod diameter (k). Hot-wire anemometry is used to measure the streamwise velocity and the mean statistics are compared against previously reported smooth wall results over a large range of Reynolds (Re) number (Marusic *et al.*, 2015) and the atmospheric surface layer (ASL) data of Metzger *et al.* (2007). The main motivation of this study is to understand the differences/similarities between a high Re smooth wall boundary layer and an approximately self-preserving rough wall boundary layer. It is found that the smooth and rough wall turbulent boundary layers present some similarities at low Re . However, as Re increases, they have different asymptotic behaviours. In the present surface roughness ($p = 8k$), the viscous drag becomes negligible in comparison to the form drag as Re increases, thereby allowing the entire turbulent boundary layer to evolve in a practically self-preserving manner. Further, it is observed that beyond a critical Re the entire boundary layer complies with Townsend's Reynolds number similarity (Townsend, 1956). These results contrast with those of a smooth wall boundary layer where self-preservation and the Reynolds number similarity are satisfied only in the outer region and at infinitely large Re . Altogether, the present study strongly suggests that while the smooth wall TBL will eventually approach its Re -independent asymptotic state only when $Re \rightarrow \infty$, the rough wall TBL reaches its asymptotic state at a faster rate and at finite Re .

INTRODUCTION

The structure of a zero pressure gradient turbulent boundary layer (hereafter denoted ZPG TBL) over a smooth wall has been the subject of a large number of comprehensive studies over many decades (Clauser, 1956; Rotta, 1962; Kline *et al.*, 1967; Robinson, 1991; Gad-el Hak & Bandyopadhyay, 1994; Jiménez, 2004; Klewicki, 2010; Marusic *et al.*, 2010; Smits *et al.*, 2011). Several aspects of the ZPG TBL were investigated, *e.g.* turbulence production, coherent structures, interaction between the inner and outer regions, from both fundamental and engineering viewpoints. From a fundamental point of view, two important questions are still being pursued rigorously, namely, i) can a ZPG TBL evolve in a self-preserving manner? ii) what is the effect of the Reynolds number (Re) on its structure?

Self-preservation (hereafter denoted SP) assumes that all normalised (or scaled) distributions of mean quantities (*e.g.* mean velocity and Reynolds stresses) have similar shapes at all stages of development of the flow. SP requires only one set of velocity and length scales. Townsend (1956) showed that a ZPG TBL cannot be in SP over a smooth wall at finite Re because of the presence of viscous dominated near-wall region. Only when $Re \rightarrow \infty$ can SP be envisaged. However, from an experimental point of view, if one increases Re to infinitely large values, the TBL cannot be considered as developing over smooth wall. This is because the thickness of the viscosity dominated near-wall layer decreases as Re increases. It is then expected that at some critical value of Re , the thickness of this layer would become so small that the imperfections of the surface would act as roughness and the wall can no longer be considered smooth.

Recently, Talluru *et al.* (2016) carried out a SP analysis of a zero pressure gradient (ZPG) turbulent boundary layer over smooth and rough walls. They confirmed that it is not possible to obtain complete SP on a smooth wall, except when $Re \rightarrow \infty$. Complete SP refers to similarity across the entire boundary layer while partial SP refers to similarity in a limited portion of the boundary layer. In the current study, we focus primarily on the former case and we drop the term "complete" in the rest of the paper for convenience. On the other hand, Rotta (1962); Townsend (1956); Talluru *et al.* (2016) showed that SP can be obtained over certain rough walls. This is possible when the viscous drag is negligible by comparison to the form drag. In such a case, the boundary layer is effectively independent of viscosity and ultimately Re . Further, they showed that the SP requirements are $u_o = \text{constant}$, $l_o \sim x$ and $k/l_o = \text{constant}$ (u_o and l_o are the velocity and length scales respectively and k is the roughness height), which are supported by experimental results. In particular, they showed that a turbulent boundary layer over a 2D rough wall made up of transverse bars with k increasing linearly with x (Kameda *et al.*, 2008) satisfies SP.

It is because SP of a ZPG TBL is presumed to be attainable at very large Reynolds numbers that ZPG TBLs are continually studied at increasingly larger Re . Such studies are believed to help us gain some insight into how the TBL approaches its asymptotic state when $Re \rightarrow \infty$. This state corresponds to the case where the effect of viscosity is negligible everywhere within the boundary layer, making the TBL effectively independent of viscosity. Reaching a very large value of Re is extremely difficult both numerically

and experimentally. Note that, as mentioned above, it will not be possible for a smooth wall TBL to be tested in a laboratory when $Re \rightarrow \infty$. The concept of a TBL developing over an ideally smooth wall at a very large Reynolds number can only be considered from a numerical point of view. Unfortunately, this cannot be envisaged for the near future due to insufficient computing power.

The present paper reports measurements in a ZPG TBL over a rough wall at several Reynolds numbers. The aim of the study is to assess the behaviour of this boundary layer as Re increases and compare it with that observed over a smooth wall with the view to reappraising the asymptotic state of the turbulent boundary layer. The rough wall consists of 2D transverse round bars and is similar to that of Kamruzzaman *et al.* (2015). The reason we selected this type of rough wall is because Leonardi *et al.* (2003, 2015) and Kamruzzaman *et al.* (2015) found that the viscous drag is negligible. Thus, in essence, the boundary layer over this particular surface is independent of viscosity, as indicated by the Re -independence of its friction coefficient (Kamruzzaman *et al.*, 2015).

EXPERIMENTAL DETAILS

Experiments are conducted in a boundary layer wind tunnel which is described in detail in Krogstad *et al.* (1992) and Kamruzzaman *et al.* (2015). The test section is 5.4 m long, 0.9 m wide and 0.15 m high. The pressure gradient is maintained to be within $\pm 0.1\%$ of the free stream dynamic pressure. The rough wall consists of a periodic arrangement of cylindrical rods mounted on the wall and spanning across the full width of the test section. The diameter of the rods is nominally 1.6 mm and the spacing (p) between the rods is set at $p = 8k$. The friction velocity U_τ is obtained by integrating the pressure distribution around the roughness element (see Kamruzzaman *et al.*, 2015, for full details).

Hot-wire anemometry is used to measure the streamwise velocity fluctuations. The single-wire probe is a slightly modified Dantec 55P15 type sensor and has a spacing of 1.5 mm with a $2.5 \mu\text{m}$ diameter Wollaston Pt wire soldered between the prongs. The etched sensor length of the hot-wire is 0.5 mm giving a length to diameter ratio of 200. The inner-normalised sensor length (l^+) in these experiments varied between 3.5 and 35.6. The single-wire probe is operated with an in-house constant temperature anemometer at an overheat ratio of 1.8. For most of the measurements, the filter cut-off frequency is set at 16 kHz and the data is sampled at 35 kHz for about 120 seconds.

Hotwire is calibrated *in situ* before and after every experiment in the undisturbed free-stream flow over a velocity range of 0.2 m/s and 22 m/s. Any drift in the hotwire voltage during the course of an experiment is corrected using the linear interpolation scheme between pre- and post-calibrations described in Talluru *et al.* (2014b).

RESULTS

Mean Velocity

Figure 1 shows the normalised distributions of U in the rough wall TBL over a range of Re , where viscous length and velocity scales are used for normalisation. For comparison, the data for high Reynolds number smooth turbulent boundary layers (Marusic *et al.*, 2015), the ASL data of Metzger *et al.* (2007) and the rough wall data of Kameda *et al.* (2008) are also shown in figure 1. The rough wall studied by Kameda *et al.* (2008) consisted of square transverse bars with linearly increasing roughness ($k \propto x$) which ensured that the boundary layer satisfies self-preservation across the entire boundary layer (Talluru *et al.* (2016)). Note that the velocity profiles (over the current 2D rough wall) shown in figure 1 are measured at a fixed streamwise location and Re is varied by changing the free-stream velocity. See table 1 for details.

Relative to the smooth wall, the rough wall mean velocity distributions exhibit the expected downward shift due to increased friction velocity U_τ . In our measurements, as Re increases, the magnitude of the downward shift reaches a maximum and becomes independent of Re as observed by the constancy of U_{max}^+ , or equivalently, a constant skin friction, C_f , since $C_f = 2/U_{\text{max}}^{+2}$. As Re increases, the rough wall profiles shift to the right (higher y^+), primarily due to the use of the inner normalisation for y , reflecting the gradual increase of U_τ . The data of Kameda *et al.* (2008) also show that the mean velocity profile remains unchanged but shifted towards higher y^+ as Re increases. This is also observed in the 2D rough wall data of Krogstad & Efros (2012) and sand-grain roughness data of Squire *et al.* (2016). The ASL mean velocity profile shows a modest downward shift, which indicates that the ASL is more akin to a TBL over a rough surface than over a smooth wall. This is further supported by the magnitude of k_s^+ (the inner-normalised equivalent sand-grain roughness), which was estimated to be about 40 suggesting that the ASL is in the transitionally rough regime. For the present rough wall, k_s^+ is in the range of 45 and 770 covering both transitionally rough and fully rough regimes.

In order to see that rough wall mean velocity profiles remain unchanged once U_∞^+ becomes constant, we remove the systematic y -shift by plotting U^+ as a function of y^+/k^+ (in a log scale the ratio y^+/k^+ amounts to shifting $\log(y^+)$ by $-\log(k^+)$) as shown in figure 2. Only the profiles for which U_∞^+ remains constant are reproduced here. Although the ratio y^+/k^+ is irrelevant for the smooth wall profiles, they are plotted only as a reference. We also applied the same procedure on all the profiles of Kameda *et al.* (2008). It is clearly evident that the rough wall profiles collapse well onto a single curve of the form $U^+ = F(y^+/k^+)$ across the entire boundary layer thickness. However, it can be seen that each set of data collapses onto a different curve reflecting the different value of C_f . This Re -independence of the normalised velocity profiles conform that the Reynolds number similarity is achieved in the present rough wall (k is constant) and that of Kameda *et al.* (2008) (i.e., $k \propto x$).

Figure 3 shows the mean velocity profiles at several x positions for the smooth (Marusic *et al.*, 2015) and the rough wall boundary layers, normalised by wall units. As expected, there is no collapse of mean velocity profiles for the smooth wall, in particular, U_∞^+ keeps increasing, reflecting the decreasing value of U_τ with x . On the other hand, there is a good collapse for the rough wall boundary layers. This shows that even in the present case where the roughness height is constant with x , SP is well achieved across the entire boundary layer over the streamwise fetch used in this study. These results are consistent with the SP analysis of Talluru *et al.* (2016) who showed that U_τ cannot be a scaling velocity for the smooth wall as it violates one of the SP conditions, i.e., the scaling velocity must be constant with x . It should be stressed that Talluru *et al.* (2016) showed that SP requirements also imposes that $k \propto x$, which is not the case for the present rough wall, thus limiting the achievement of SP only for streamwise distances over which C_f remains approximately constant. Interestingly, Townsend (1956) states that “if, as must be assumed, Reynolds number similarity of self-preserving flows exists, the form of the self-preserving functions are universal for any one type of flow”. The present rough wall measurements shown in figures 2 and 3 illustrate this statement rather well. This is further confirmed when the velocity profiles shown in figure 2 are replotted as function of y/δ (not shown here). For both rough walls, the profiles show similar collapse as in figure 2, while the two smooth wall velocity distributions are very different from one another. Altogether, the results presented so far confirm that the Reynolds number similarity can be achieved *everywhere* within a rough wall TBL at a finite Reynolds number, but not in a smooth wall TBL, where it is expected to be observed in its outer region at

x	Sym.	Re_τ	Re_θ	U_∞	ν/U_τ	U_τ	δ_{99}	δ^*	θ	l^+	k_s^+	δ/k	δ/k_s
m				(ms^{-1})	(μm)	(ms^{-1})	(m)	(m)	(m)				
<u>fixed x</u>													
2.54	○	629	1760	2.07	142	0.108	0.089	0.022	0.013	3.5	47	56	13.4
2.54	◇	1020	2750	3.03	92.8	0.166	0.094	0.024	0.014	5.4	103	59	9.9
2.54	△	1516	3922	4.17	64.6	0.238	0.098	0.026	0.015	7.7	220	61	6.9
2.54	□	2340	6045	6.43	41.0	0.381	0.096	0.026	0.015	12.2	299	62	7.8
2.54	×	3945	9925	10.40	25.1	0.623	0.099	0.026	0.015	19.8	450	62	8.7
2.54	*	5766	14305	15.00	17.4	0.900	0.100	0.025	0.015	28.7	625	63	9.2
2.54	+	7170	17780	18.80	14.0	1.127	0.101	0.025	0.015	35.6	767	63	9.3
<u>different x</u>													
1.94	○	5130	12870	16.11	16.0	0.966	0.082	0.022	0.012	31	650	52	7.9
2.24	◇	5652	13810	16.02	16.2	0.961	0.091	0.023	0.013	30.8	651	57	8.7
2.54	△	6250	15130	15.90	16.2	0.948	0.102	0.025	0.015	30.6	651	63	9.6
2.84	□	6588	15880	15.57	16.6	0.934	0.109	0.026	0.016	30.1	651	68	10.1
3.14	×	7140	16310	15.85	16.2	0.951	0.116	0.026	0.016	30.7	651	73	10.9

Table 1. Experimental parameters over the 2D rough wall.

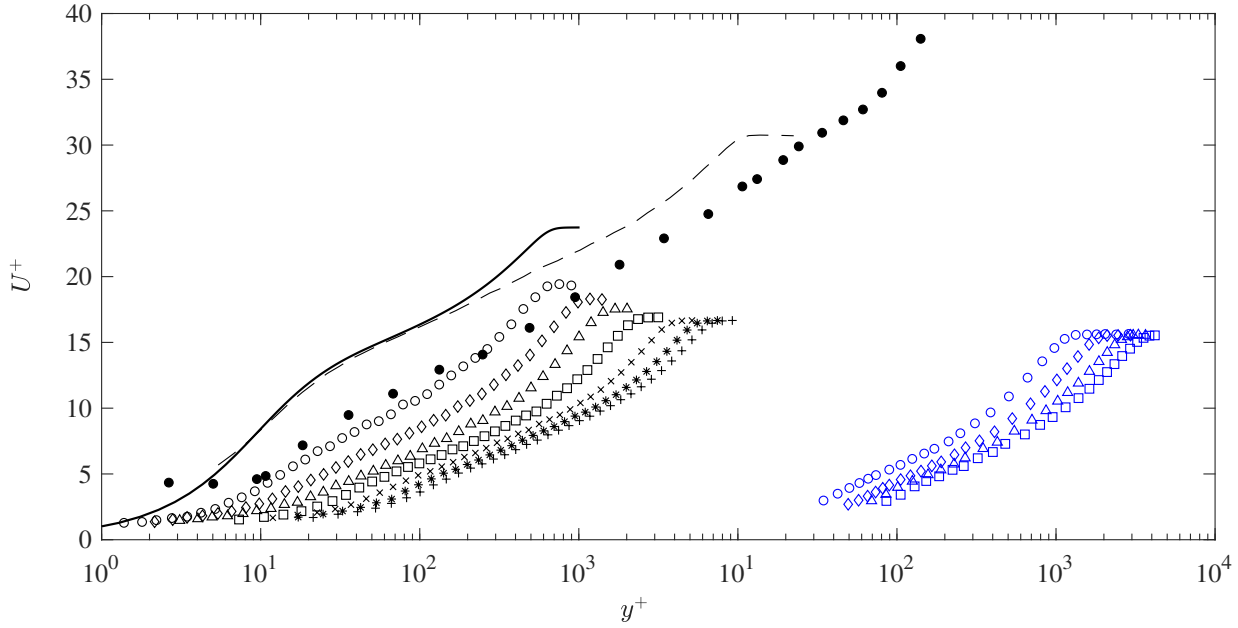


Figure 1. Mean velocity profiles over 2D rough wall at several Re for a fixed streamwise location. The data are normalised by the wall units; $d_o = 0.48k$. Solid line - smooth wall DNS data (Schlatter & Örlü, 2010, $Re_\tau = 674$); dashed lines - smooth wall (Marusic *et al.*, 2015, $Re_\tau \approx 13000$); open symbols: present data; filled black circles: ASL data (Metzger *et al.*, 2007, $Re_\tau = 7.8 \times 10^5$); open blue symbols: (Kameda *et al.*, 2008, $1300 \leq Re_\tau \leq 3900$).

an infinitely large Re .

Longitudinal Reynolds Stress

The distributions of the normalised longitudinal Reynolds stress, $\overline{u^{2+}}$, are reported in figure 4 for a TBL over a smooth wall, the present rough wall and the ASL. The smooth wall distributions show the characteristic near-wall peak which seems to increase in

magnitude with Re . There is also an increase in $\overline{u^{2+}}$ in the outer region of the boundary layer. On the rough wall, the near-wall peak gradually decreases before practically disappearing as Re increases, while the outer part of the distribution increases, seemingly approaching a limiting distribution. The ASL distribution resembles more to the laboratory rough wall TBL distributions at lower Re (*i.e.*, transitionally rough regime), where we observe an inner

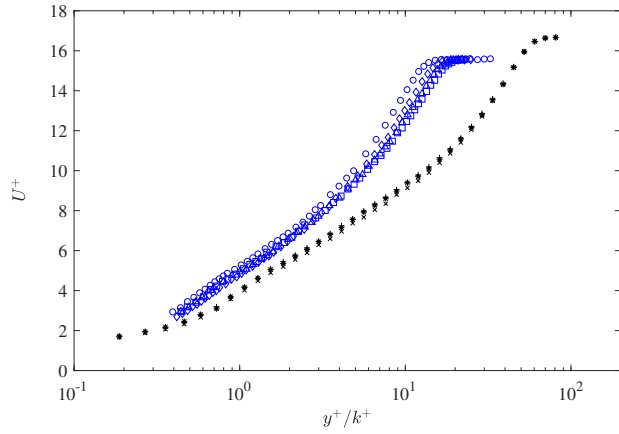


Figure 2. Mean velocity profiles as a function of y^+/k^+ at several Re for a fixed streamwise location. Symbols same as in figure 1. Only the profiles for which U_∞^+ remains constant are reported. The smooth wall profiles (U^+ vs y^+) are shown for reference only.

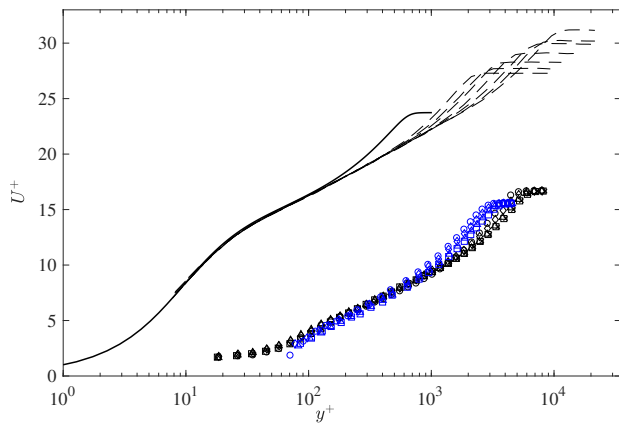


Figure 3. Mean velocity profiles at several streamwise locations on smooth and rough walls for the nominally fixed free-stream velocity U_e . Symbols: present rough wall measurements ($1.94 \leq x \leq 3.14$); dashed lines: smooth wall data at different x given in [Marusic et al. \(2015\)](#); solid line: smooth wall DNS data ([Schlatter & Örlü, 2010](#), $Re_\tau = 674$).

peak and an outer peak. Notice that if the shift in y^+ (due to the use of viscous length scale for normalising y) is accounted for, one can argue that the rough wall distributions approach a limiting distribution. This is shown in figure 5 where we plot our data with those of [Kameda et al. \(2008\)](#) as function of y^+/k^+ . Similar to the mean velocity distributions in figure 2, the turbulence intensity profiles collapse onto distinctive distributions. A similar collapse is also observed when plotted the data as function of y/δ (not shown here) but not as expected for the smooth wall data.

CONCLUSIONS

Hotwire measurements in a ZPG TBL over a 2D rough wall ($p = 8k$) at several Reynolds numbers have been carried out in a wind tunnel with the view of assessing the behaviour of a ZPG TBL as the Reynolds number increases. Several observations associated with an increasing Re have been made:

(i) Over the streamwise fetch of the measurements, a rough wall boundary layer quickly approaches a Re -independent asymptotic state as indicated by the constancy of the ratio U_∞/U_τ (or C_f) with respect to Reynolds number and the collapse of wall-unit nor-

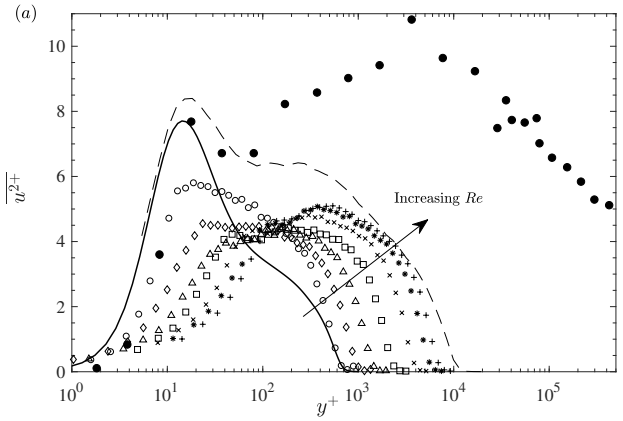


Figure 4. Profiles of $\overline{u^{+2}}$ in a TBL over a smooth wall and the 2D rough wall at several Re for a fixed x position. The data are normalised by the wall units. Smooth wall: solid line ([Schlatter & Örlü, 2010](#), $Re_\tau = 674$), dashed line ([Talluru et al., 2014a](#), $Re_\tau = 15000$); filled circles: ASL data ([Metzger et al., 2007](#), $Re_\tau = 7.8 \times 10^5$); Rough wall: black symbols with Re_τ ranging between 620 and 7200.

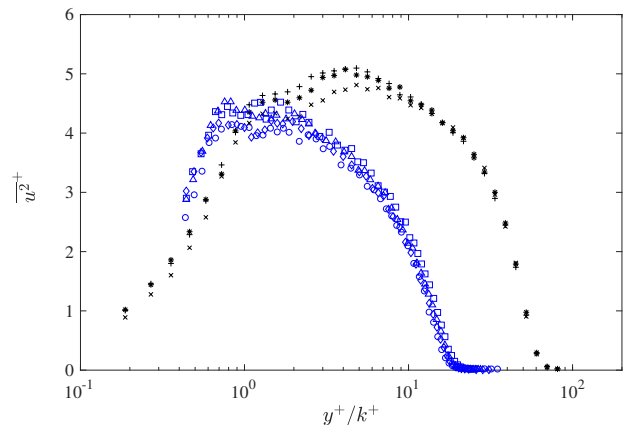


Figure 5. Profiles of $\overline{u^{+2}}$ in smooth and rough wall TBLs at several Re , as function of y^+/k^+ . The data are normalised by wall units. Symbols same as in figure 2.

malised mean velocity and velocity variance profiles. For a smooth wall turbulent boundary layer, U_∞/U_τ increases indefinitely with Reynolds number.

(ii) The inner peak of the longitudinal velocity variance, which is observed over a smooth wall, gradually disappears on the rough wall, while an outer peak emerges and becomes more pronounced. On the smooth wall, the inner peak seems to remain as Re increases although an outer peak emerges.

(iii) The constancy of C_f with respect to Re implies that the drag is solely composed of the form drag generated by the roughness elements while the viscous drag is practically eliminated or negligible when compared to the form drag.

These observations indicate that the ZPG TBL over a rough surface, where the viscous effect is negligible *everywhere*, becomes Re -independent, thus satisfying Townsend's Reynolds number similarity at relatively low to moderate Reynolds numbers. This behaviour differs from that of a smooth wall ZPG TBL where the Reynolds number similarity is believed to be approximately satisfied at very high Reynolds numbers and only in the outer part of the boundary layer.

REFERENCES

- Clauser, F. H. 1956 The turbulent boundary layer. *Adv. App. Mech.* **4**, 1–51.
- Gad-el Hak, M & Bandyopadhyay, P. R. 1994 Reynolds number effects in wall-bounded turbulent flows. *Appl. Mech. Rev.* **47** (8), 307–365.
- Jiménez, J. 2004 Turbulent flows over rough walls. *Annu. Rev. Fluid Mech.* **36**, 173–196.
- Kameda, T., Mochizuki, S., Osaka, H. & Higaki, K. 2008 Realization of the turbulent boundary layer over the rough wall satisfied the conditions of complete similarity and its mean flow quantities. *J. Fluid Sci. Tech.* **3** (1), 31–42.
- Kamruzzaman, Md, Djenidi, L, Antonia, R. A. & Talluru, K. M. 2015 Drag of a turbulent boundary layer with transverse 2d circular rods on the wall. *Exp. Fluids* **56** (6), 1–8.
- Klewicki, J. C 2010 Reynolds number dependence, scaling, and dynamics of turbulent boundary layers. *J. Fluids Eng.* **132** (9), 094001.
- Kline, S. J., Reynolds, W. C., Schraub, F. A. & Runstadler, P. W. 1967 The structure of turbulent boundary layers. *J. Fluid Mech.* **30** (04), 741–773.
- Krogstad, P-Å, Antonia, R. A. & Browne, L. W. B. 1992 Comparison between rough-and smooth-wall turbulent boundary layers. *J. Fluid Mech.* **245**, 599–617.
- Krogstad, P-Å & Efros, V. 2012 About turbulence statistics in the outer part of a boundary layer developing over two-dimensional surface roughness. *Phys. Fluids* **24** (7), 075112.
- Leonardi, S., Orlandi, P., Djenidi, L. & Antonia, R. A. 2015 Heat transfer in a turbulent channel flow with transverse square bars circular rods on one wall. *J. Fluid Mech.* **776**, 512–530.
- Leonardi, S., Orlandi, P., Smalley, R. J., Djenidi, L. & Antonia, R. A. 2003 Direct numerical simulations of turbulent channel flow with transverse square bars on one wall. *J. Fluid Mech.* **491**, 229–238.
- Marusic, I., Chauhan, K. A., Kulandaivelu, V. & Hutchins, N. 2015 Evolution of zero-pressure-gradient boundary layers from different tripping conditions. *J. Fluid Mech.* **783**, 379–411.
- Marusic, I., McKeon, B. J., Monkewitz, P. A., Nagib, H. M., Smits, A. J. & Sreenivasan, K. R. 2010 Wall-bounded turbulent flows at high Reynolds numbers: Recent advances and key issues. *Phys. Fluids* **22** (6), 065103.
- Metzger, M., McKeon, B. J. & Holmes, H. 2007 The near-neutral atmospheric surface layer: turbulence and non-stationarity. *Phil. Trans. R. Soc. A* **365** (1852), 859–876.
- Robinson, S. K. 1991 Coherent motions in the turbulent boundary layer. *Ann. Rev. Fluid Mech.* **23** (1), 601–639.
- Rotta, J. C. 1962 Turbulent boundary layers in incompressible flow. *Prog. Aero. Sci.* **2** (1), 1–95.
- Schlatter, P. & Örlü, R. 2010 Assessment of direct numerical simulation data of turbulent boundary layers. *J. Fluid Mech.* **659**, 116–126.
- Smits, A. J., McKeon, B. J. & Marusic, I. 2011 High-Reynolds number wall turbulence. *Ann. Rev. Fluid Mech.* **43**, 353–375.
- Squire, D.T., Morrill-Winter, C., Hutchins, N., Schultz, M.P., Klewicki, J.C. & Marusic, I. 2016 Comparison of turbulent boundary layers over smooth and rough surfaces up to high Reynolds numbers. *J. Fluid Mech.* **795**, 210–240.
- Talluru, K. M., Baidya, R., Hutchins, N. & Marusic, I. 2014a Amplitude modulation of all three velocity components in turbulent boundary layers. *J. Fluid Mech.* **746**, R1.
- Talluru, K. M., Djenidi, L., Kamruzzaman, Md. & Antonia, R. A. 2016 Self-preservation in a zero pressure gradient rough wall turbulent boundary layer. *J. Fluid Mech.* **788**, 57–69.
- Talluru, K. M., Kulandaivelu, V., Hutchins, N. & Marusic, I. 2014b A calibration technique to correct sensor drift issues in hot-wire anemometry. *Meas. Sci. Tech.* **25** (10), 105304.
- Townsend, A. A. 1956 *The Structure of Turbulent Shear Flow*. C. U. P.